Molecular Biology of the Cell
Vol. 11, 1275–1291, April 2000

The *Dictyostelium* LIM Domain-containing Protein LIM2 Is Essential for Proper Chemotaxis and Morphogenesis

Sharon Chien,* Chang Y. Chung,* Sujatha Sukumaran,† Nicholas Osborne,* Susan Lee,* Charlene Ellsworth,* James G. McNally,†‡ and Richard A. Firtel*§

*Section of Cell and Developmental Biology, Division of Biology, Center for Molecular Genetics, University of California, San Diego, 9500 Gilman Drive, La Jolla, California 92093-0634; and †Department of Biology, Washington University, St. Louis, Missouri 63130

Submitted November 11, 1999; Revised January 12, 2000; Accepted January 19,2000
Monitoring Editor: Peter N. Devreotes

We have identified *limB*, a gene encoding a novel LIM domain-containing protein, LIM2, in a screen for genes required for morphogenesis. *limB* null cells aggregate, although poorly, but they are unable to undergo morphogenesis, and the aggregates arrest at the mound stage. *limB* null cells exhibit an aberrant actin cytoskeleton and have numerous F-actin–enriched microspikes. The cells exhibit poor adhesion to a substratum and do not form tight cell–cell agglomerates in suspension. Furthermore, *limB* null cells are unable to properly polarize in chemoattractant gradients and move very poorly. Expression of *limB* from a prestalk-specific but not a prespore-specific promoter complements the morphogenetic defects of the *limB* null strain, suggesting that the *limB* null cell developmental defect results from an inability to properly sort prestalk cells. LIM2 protein is enriched in the cortex of wild-type cells, although it does not colocalize with the actin cytoskeleton. Our analysis indicates that LIM2 is a new regulatory protein that functions to control rearrangements of the actin cytoskeleton and is required for cell motility and chemotaxis. Our findings may be generally applicable to understanding pathways that control cell movement and morphogenesis in all multicellular organisms. Structure function studies on the LIM domains are presented.

INTRODUCTION

Multicellular development in *Dictyostelium discoideum* involves the chemotaxis of up to 10^5 individual cells to form a multicellular aggregate. The ligand for chemotaxis is extracellular cAMP that activates a series of second messenger pathways through cAMP, G protein-coupled, serpentine receptors that result in the reorganization of the actin/myosin cytoskeletons and directed movement of cells toward the aggregation center (Parent *et al.*, 1998; Aubry and Firtel, 1999). Cell-type differentiation and morphogenesis ensue with the sorting of prestalk cells to the apical region of the mound to form a tip and establish the initial spatial patterning of the prestalk and prespore cell populations. The tip elongates to form a first finger that falls over, producing a migrating slug or pseudoplasmodium (Loomis, 1982). Culmination leads to the formation of a mature fruiting body containing spores and stalk cells. Cell sorting during tip formation and subsequent morphogenesis is thought to be mediated, at least in part, by differential chemotaxis to cAMP via similar chemotaxis pathways and differential cell adhesion (Mee *et al.*, 1986; Traynor *et al.*, 1992; Early *et al.*, 1995; Spudich *et al.*, 1995; Levine *et al.*, 1997; Chen *et al.*, 1998; Ginger *et al.*, 1998; Nicol *et al.*, 1999).

Relatively little is understood about the cellular processes and molecular mechanisms that control cell movements during cell sorting and morphogenesis in multicellular organisms. To better understand the pathways involved, we undertook a genetic screen to identify genes required for these processes. One of the genes that we identified is *limB*, encoding the protein LIM2, which contains five LIM domains. *limB* is preferentially expressed during aggregation and mound formation. *limB* null cells are unable to properly polarize or chemotax in cAMP gradients and arrest development at the tight mound stage. The LIM family of proteins, named for the founding members lin-11, isl1, and mec-3, is a group of proteins containing at least one zinc

‡ Present address: Laboratory of Receptor Biology and Gene Expression, National Cancer Institute, National Institutes of Health, Bethesda, MD 20892.
§ Corresponding author. E-mail address: rafirtel@ucsd.edu.

binding "LIM" domain with the primary structure $CX_2CX_{16-23}CX_2CX_{16-23}CX_2C$ that function as domains for protein–protein interactions. LIM domain-containing proteins were discovered as genes required for proper development in two disparate systems: *lin-11* and *mec-3*, which are involved in *Caenorhabditis elegans* vulval cell and mechanosensory neuron development, respectively (Way and Chalfie, 1988; Freyd *et al.*, 1990), and *isl1*, which is necessary for proper neuronal and endocrine development in vertebrates (Karlsson *et al.*, 1990; Thor *et al.*, 1991; Inoue *et al.*, 1994; Pfaff *et al.*, 1996; Ahlgren *et al.*, 1997). Several cytoplasmic LIM domain-containing proteins control cytoskeletal rearrangements, including paxillin, LIM kinase, Zyxin, cCrp, and the *Dictyostelium* LIM domain protein DdLim1, which is required for proper protrusion of lamellipodia during chemotaxis (Sadler *et al.*, 1992; Schmeichel and Beckerle, 1994; Brown *et al.*, 1996; Prassler *et al.*, 1998; Edwards *et al.*, 1999).

The work described in this article indicates that *limB* null cells are unable to properly organize their actin cytoskeleton or polarize in a chemoattractant gradient, leading to specific defects in cell motility and an inability to properly chemotax and undergo morphogenesis. Our studies provide new insights into the regulatory pathways required for cell sorting during morphogenesis in multicellular organisms.

MATERIALS AND METHODS

Cell Biology, Development, and Staining

Wild-type strain KAx-3 *Dictyostelium* cells were grown and transformed using standard techniques (Nellen *et al.*, 1987). Clonal isolates of strains carrying expression constructs were selected on DM agar containing 20–60 μg/ml G418 in association with neomycin resistant *Escherichia coli* strain B/r (Hughes *et al.*, 1992). To examine morphology of development, cells were plated at varying densities on 12 mM Na/KPO_4 (pH 6.1) containing agar plates.

For β-galactosidase staining, cells were developed on nitrocellulose filters resting on the top of nonnutrient agar plates and then stained as described previously (Mann *et al.*, 1994). Staining of slugs with the Mitotracker Green (Molecular Probes, Eugene, OR) vital stain was accomplished by mixing one part labeled strain with three parts unstained strain. Of the cells from the strain to be labeled, 25% were washed in Na/KPO_4 buffer and placed on ice in 5 μM Mitotracker Green in Na/KPO_4 buffer for 30 min. These cells were washed again and mixed with the remaining cells to be plated. A total of 3×10^7 cells were plated onto agar containing 12 mM Na/KPO_4 (pH 6.1) in a 60 mm plastic Petri dish. Fluorescence images of slugs were taken with a 10× objective. All fluorescence images were collected on a Photometrics Sensys camera, using IP Lab Spectrum software (Scanalytics, Fairfax, VA).

Cell pulsing and induction using cAMP were performed as follows. Axenically grown HL5 cultures were washed and resuspended at 4×10^6 cells/ml in 12 mM phosphate buffer and pulsed with ~30 nM cAMP every 6 min, using a multistaltic pump. Pulsing was done for >4.5 h at 230 rpm shaking speed. For induction with high cAMP, cells were pulsed as above for 5 h and then shaken at 120 rpm (slow speed) and induced twice in 3 h with ~300 μM cAMP. After this, cAMP was replenished with the addition of 300 μM cAMP every 2 h. For Northern blot analysis of these experiments, 5×10^7 cells were taken for each sample. Clumping was analyzed by adding 10–15 μl of cells to 2.5 μl of 50% glycerol in 12 mM Na/KPO_4 and dropping them onto microscope slides.

Western blot analysis and fluorescence staining were performed as described previously (Chung and Firtel, 1999).

Isolation of the limB Mutant

Mutagenesis was performed using the REMI method (Kuspa and Loomis, 1992) using the restriction enzyme *Dpn*II in combination with a *Bam*HI linearized pUCBsr-ΔBam. Mutagenized cells were plated on SM agar with *Klebsiella aerogenes* as a food source and developed. Clones were screened for those that were unable to develop past the mound stage. Such strains could be defective in the ability to undergo morphogenesis, such as sorting of the prestalk cells to the anterior, or in cell-type differentiation.

limB interrupted cells were identified as one of the strains that arrested at the mound stage (did not form a tipped aggregate on SM agar plates). Plasmid rescue was performed by digesting genomic DNA isolated from this clonal line with *Eco*RI and religating (Kuspa and Loomis, 1992; Dynes *et al.*, 1994). The resultant vector was used to recapitulate the mound-arrest phenotype in the KAx-3 background by recutting the rescued plasmid with *Eco*RI and transforming it into wild-type cells. Disruption of the gene by homologous recombination was assayed by Southern blot analysis of genomic DNA (Nellen *et al.*, 1987). Several clones were picked, and all exhibited indistinguishable phenotypes. A single clone was chosen for the work described here.

Molecular Biology

The full sequence of *limB* was obtained by using a partial sequence obtained from the rescued REMI plasmid as a probe to screen a λZAP cDNA library described previously (Schnitzler *et al.*, 1995). cDNA clones were isolated and sequenced.

To obtain a clone of the complete ORF, the regions flanking the vector in the recovered plasmid were used to screen a *Dictyostelium* cDNA library. In this screen, we obtained clones containing the AUG initiation codon but never obtained the region encoding the C terminus of the protein and the termination codon. This is probably due to the presence of a high number of codons for lysine and glutamic acid residues near the C terminus, which may act as the binding site for oligo(dT) during library construction, because the sequence is very rich in A residues and mimics the 3′ terminal poly(A) of mRNAs. The C terminus was obtained by cloning a genomic fragment, which contained part of the ORF and the UAA termination codon of LIM2 (our unpublished results).

All *limB* constructs were expressed as stable G418-resistant transformants downstream from the *Act15*, prespore-specific *SP60* promoter, or the prestalk-specific *ecmAO* promoter as described previously (Dynes *et al.*, 1994). Deletion constructs were created using either endogenous restriction sites or internal primers located at the positions indicated in Table 1. Site-directed mutagenesis was carried out using the Transformer Site Directed Mutagenesis Kit from Clontech (Cambridge, UK). For the mutant Y45F, the mutation primer used was (5′-CATTTGGATCTTTAAATGTAAGATATGTTGGTGC-3′). For the C290S mutant, the mutation primer was (5′-CACGTAACTTGTCACCACTACCTGAACTTGAGAAACACTCTGG-3′). The mutation primer for C414S was (5′-CCAGCGAATGGTACTTGACTAGTGGTACTAGTGAAATGTTCTGG-3′). The constructs containing these point mutations were sequenced to verify the proper substitutions and determine the absence of any other mutations. For expression of myc-tagged LIM2, PCR was carried out with the sense (5′-GTTTTTACTAGTAAAAAAATGGAACAAAAATTAATTTCAGAAGAAGATTTAAATGCAAATAAAAATGTATTATCAG-3′) and the antisense (5′-CATGACAAGTTTTACCCAC-3′) using the *limB* cDNA as a template. The resulting fragment was cut with *Eco*RI–*Spe*I. The PCR, sense (5′-GTTTTTGGATCCGTAAGATTGCAAGACAAAAACG-3′), and antisense (5′-GTTTTTCTCGAGAAATTAAGCTTCAGCTTTTTTTATCACC-3′) with *LIM2* cDNA as a template, were cut with *Eco*RI–*Xho*I, and both were cloned into pBSK(+) (Stratagene, La Jolla, CA) *Eco*RI–*Spe*I and *Xho*I–*Eco*RI, respectively, for sequencing. These two fragments were ligated together into an expression vector. The green fluorescent protein (GFP)-tagged LIM2 was constructed by ligating two PCR products into expression vector l. The

first PCR was performed using *LIM2* cDNA as a template, and the primers sense (T3 primer) and antisense (5′-GTTTTTCTC-GAGAAATTAAGCTTCAGCTTTTTTATCACC-3′), and cut with *Bgl*II–*Pst*I. The second PCR used GFP-pInvitrogen (Invitrogen, San Diego, CA) as a template, with the primers sense (5′- cloning primer) and antisense (5′-GTTTTAGATCTTTTGTATAGTTCATC-CATGCCATG-3′). These products were sequenced and cloned into an expression vector cut with *Xho*I–*Spe*I. Northern blots were performed as described previously (Mann and Firtel, 1987).

Cell Motion and Chemotaxis Analysis

Analysis of chemotaxis using phase-contrast and DIC video microscopy was performed as previously described (Ma *et al.*, 1997; Chung and Firtel, 1999; Lee *et al.*, 1999; Meili *et al.*, 1999).

For examination of cell movement in multicellular aggregates, cells were allowed to settle onto a dialysis membrane laid on a coverslip kept in a humid chamber and then allowed to develop to the appropriate stage as described previously (Doolittle *et al.*, 1995). Images were recorded using a custom-modified IMT-2 Olympus (Melville, NY) inverted microscope with a scientific-grade CCD camera cooled to −0°C (Doolittle *et al.*, 1995). Depending on the desired magnification, we used either an Olympus S Plan PL 0.3 NA/10× air lens or an Olympus D Plan Apo UV 0.8 NA/20× oil immersion lens. Recorded three-dimensional (3-D) images were processed to reduce out-of-focus light by several well characterized restoration methods (Preza *et al.*, 1992; Conchello and McNally, 1996). 3-D cell tracking was performed using an upgraded version of customized software (Awasthi *et al.*, 1994).

RESULTS

Isolation and Sequencing of limB

limB, encoding the protein LIM2, was identified in a screen for mutants that arrested at the mound stage using the REMI method of insertional mutagenesis (see MATERIALS AND METHODS) (Kuspa and Loomis, 1992). Regions of the chromosome flanking the insertion were excised from the genomic DNA using plasmid rescue, and the plasmid was used to recapitulate the original REMI mutant by homologous recombination into a wild-type background as described previously (Kuspa and Loomis, 1992; Dynes *et al.*, 1994). An analysis of randomly isolated clones showed a one-to-one correlation between the mound-arrest phenotype and disruption of *limB* (our unpublished results). The cloning of the DNA encoding the complete LIM2 ORF is described in the MATERIALS AND METHODS.

The derived amino acid sequence of LIM2 is shown in Figure 1A. LIM2 shows significant homology to the family of proteins containing zinc finger-like LIM domains. LIM2 contains five LIM domains in its C terminus; its N terminus has no homology to proteins in the database. Within its LIM domains, *D. discoideum* LIM2 shows the strongest homology to vertebrate paxillin (Turner and Miller, 1994). However, LIM2 lacks a recognizable SH3 binding domain in its NH_2 terminus, a feature of paxillins (Turner and Miller, 1994), and is not detectably tyrosine-phosphorylated during development or in response to cAMP signaling (our unpublished results; see MATERIALS AND METHODS). The NH_2 terminus of LIM2 contains seven repeats of (V/I/M)S(T/S/R/K)GPGL, followed by five repeats of S(S/F)GV. Another characteristic of the LIM2 protein is the presence of a highly charged C terminus with 18 lysines and 11 glutamates in the last 50 amino acids. Many of the lysines and glutamic acids are associated in the sequences KE, EK, KKE, and KEKE.

The presence of multiple LIM domains at the C terminus and a sequence comparison of the individual LIM domains identify *LIM2* as a Group 3 LIM protein according the classification of Taira *et al.* (1995). Alignments of the LIM domains from several Group 3 LIM proteins are shown in Figure 1B. The LIM2 LIM domains show the strongest overall sequence homology to those of paxillin.

limB Null Cells Exhibit Defects in the Actin Cytoskeleton

Microscopic examination of *limB* null cells showed that they have many microspikes around the periphery of cells, suggesting an aberrant organization of the actin cytoskeleton. To examine this directly, we stained the actin cytoskeleton in *limB* null and wild-type cells with FITC-conjugated phalloidin. F-actin is found as a cortical band or concentrated at the leading edge at the site of pseudopod formation and in the posterior of polarized, aggregation-competent wild-type cells (Figure 2A). In contrast, *limB* null cells have many F-actin–enriched microspikes, which may be filopodia, along the periphery of the cells, with the remainder of the F-actin found in nondistinct patches scattered in the cytoplasm. We also examined F-actin localization in living cells by visualizing the distribution of coronin–GFP, which binds to F-actin and is used to localize F-actin in living cells (Gerisch *et al.*, 1995). The distribution of F-actin was similar to that observed using phalloidin staining of fixed cells. (Figure 2B).

Using time-lapse fluorescence microscopy of coronin–GFP, we examined the dynamics of F-actin formation in *limB* null and wild-type cells in aggregation streams. GFP–coronin–expressing *limB* null or wild-type cells were mixed with unlabeled wild-type cells, allowed to develop until the onset of aggregation, and examined by time-lapse microscopy. In such experiments, the wild-type cells provide the extracellular signaling required for aggregation in case a mutant strain is deficient in producing a needed extracellular signal or cell–cell contacts and reduces problems with forming aggregation streams caused by aggregation defects of the mutant strain. As in wild-type cells, GFP–coronin concentrates at pseudoplasmodial extensions and lamellapodial faces of *limB* null cells (Figure 2D). However, this localization is significantly less robust than that observed in wild-type cells analyzed under the same conditions (Figure 2Ca). Moreover, *limB* null cells extend pseudopodia enriched with coronin–GFP in random directions relative to the direction of cell movement, and the cells appear not to be highly polarized (see below). These results suggest that *limB* null cells have significant abnormalities in the regulation of F-actin organization.

Subcellular Localization of LIM2 Protein

We used a GFP–LIM2 fusion protein, which complements the *limB* null phenotype (our unpublished results), to examine the subcellular localization of the LIM2 protein in cells (Figure 2E). The GFP–LIM2 fusion protein shows an enriched localization to the cortical/membrane regions of wild-type cells. We observed a similar localization of LIM2 using myc-tagged LIM2 (our unpublished results). To determine whether LIM2 colocalizes with the actin cytoskeleton, we examined phalloidin staining of F-actin and GFP–LIM2

Figure 1. Sequence and analysis of the domains of LIM2. A shows the derived amino acid sequence of LIM2. The five LIM domains are shaded. The NH_2-terminal repeats are boxed, and the highly charged C-terminal stretch is underlined. B shows an alignment of the LIM domains from several Group 3 LIM domain-containing proteins. The domains are numbered with the most N-terminal domain numbered 1. The LIM domains of LIMB are aligned with all the LIM domains of chicken paxillin and the vertebrate Zyxin protein. The LIM domains of LIM2 show the strongest overall sequence homology to the LIM domains of paxillin, with the highest homology (57%) between the fourth LIM domain of LIM2 and the first LIM domain of paxillin. The PINCH LIM domain has 55% homology to the fourth LIM domain of LIM2. The other LIM domains of PINCH, however, do not show this high level of homology to any of the LIM2 LIM domains, despite similarities in the number and arrangement of the domains within these two proteins (our unpublished results).

in fixed cells. Although both F-actin and GFP–LIM2 are associated with the cell cortex, they do not colocalize (Figure 2E, see phalloidin staining). GFP–LIM2 exhibits a more uniform cortical localization.

limB Null Cells Exhibit Growth and Developmental Phenotypes

As shown in Figure 3A, *limB* null cells form normal-sized aggregates but with delayed kinetics, forming mounds at 12 h compared with 8 h for wild-type strains. *limB* null cells arrest at the mound stage without forming tips, suggesting that these cells might have difficulties in cell migration in the mound resulting in poor cell sorting and the lack of tip formation. Expression of *limB* from the constitutive *Act15* promoter complements the *limB* null developmental phenotypes, with developmental timing and morphologies similar to those of the parental wild-type strain (our unpublished results). To examine aggregation of *limB* null cells more closely, we used time-lapse video microscopy of a monolayer of *limB* null cells (Ma *et al.*, 1997; Meili *et al.*, 1999) (see MATERIALS AND METHODS). cAMP response waves are visible beginning at ~4 h of development, similar to observations of the wild-type strains (Figure 4A; our unpublished results); however, in contrast to wild-type cells shown in Figure 4A (top panels), which start to form aggregates by 6 h, *limB* null cells do not form large, discrete, stable signaling centers until 9 h, when the cells start to chemotax toward the centers (Figure 4A, bottom panels). Some of the smaller centers formed by *limB* null cells coalesce to form normal-sized centers and aggregates at 11–12 h under these conditions. There is rotation of cells around the center of the mound, as seen in the parental KAx-3 cell line (Siegert and Weijer, 1995; Kellerman and McNally, 1999), implying that the cAMP signaling pathway functions during aggregation and within the mound (Figure 4B); however, in time-lapse movies of *limB* null cells undergoing rotation in the mound, mutant cells appear to extend pseudopodia at all angles to their direction of motion, unlike wild-type cells, which remain elongated primarily along their direction of movement.

The aggregation defects described above suggest that chemotactic migration of *limB* null cells is very delayed or aberrant, leading to a delay in mound formation. To study

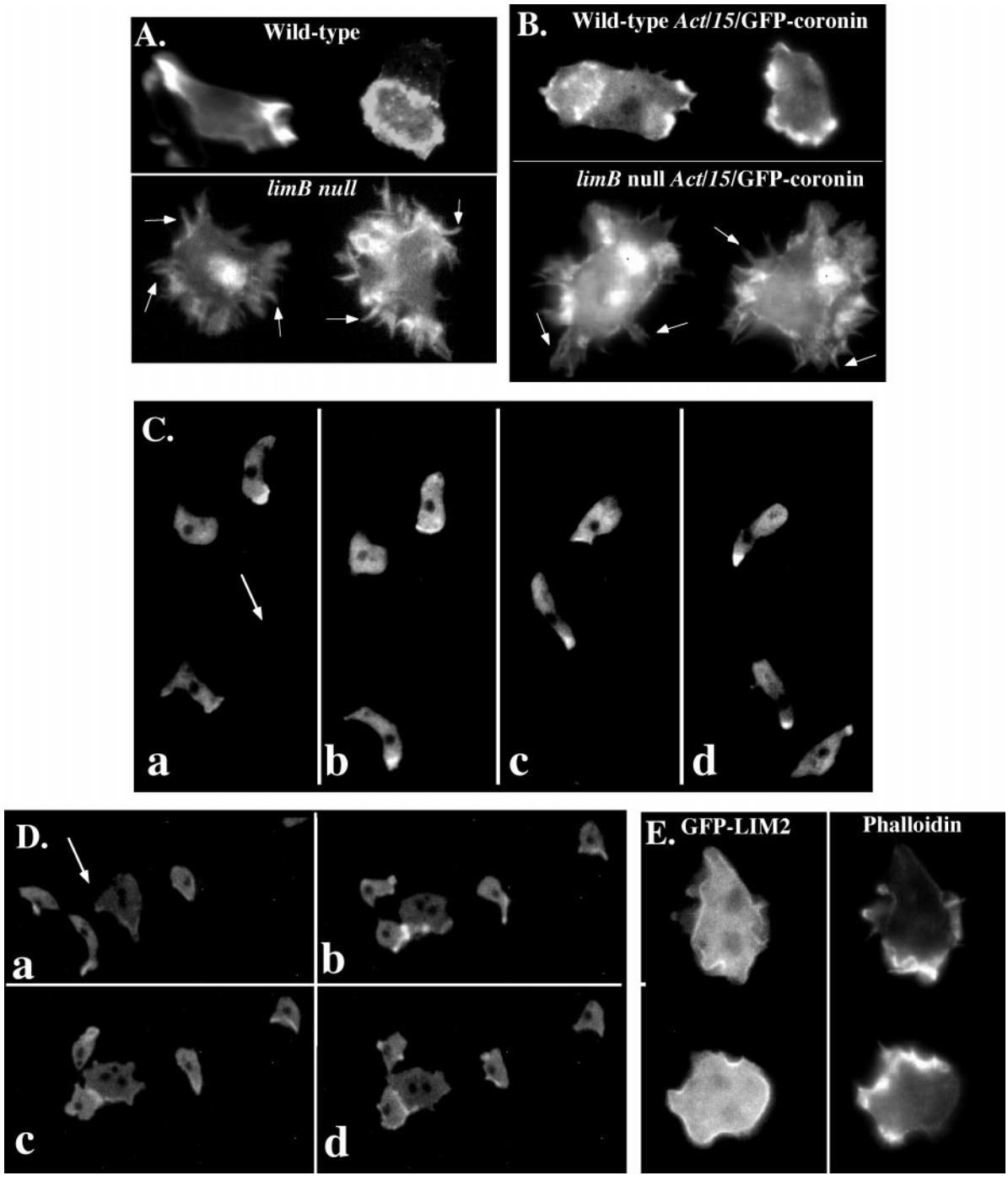

Figure 2. F-actin cytoskeletal staining and subcellular localization of LIM2. (A) *limB* null and KAx-3 cells were fixed and labeled with FITC-conjugated phalloidin to show the actin cytoskeleton as previously described (Chung and Firtel, 1999). (B) *limB* null and KAx-3 cells expressing GFP–coronin, which binds to F-actin. In both A and B, the white arrows indicate actin rich "microspike" structures observed in the *limB* null cells. C and D show the localization of F-actin in wild-type and *limB* null aggregation streams using GFP–coronin. Wild-type (C) or *limB* null (D) vegetatively growing cells expressing GFP–coronin were washed and mixed with an ~10-fold excess of unmarked wild-type cells and plated for development on thin agar. Once aggregation streams were formed, the cells were photographed using time-lapse video microscopy with either a Nikon (Melville, NY) Microphot FX or an Eclipse TE300 microscope with a 20× objective and equipped with fluorescence. The images were directly captured onto a computer using IP Labs software. Only the GFP–coronin–expressing cells can be seen. The direction of movement is indicated by the arrow. A series of sequential images are shown. E shows the subcellular localization of LIM2. LIM2–GFP fusion, which complements the null phenotype and was expressed from the *Act15* promoter, is shown in the left panel. Phalloidin staining of F-actin is shown in the right panel.

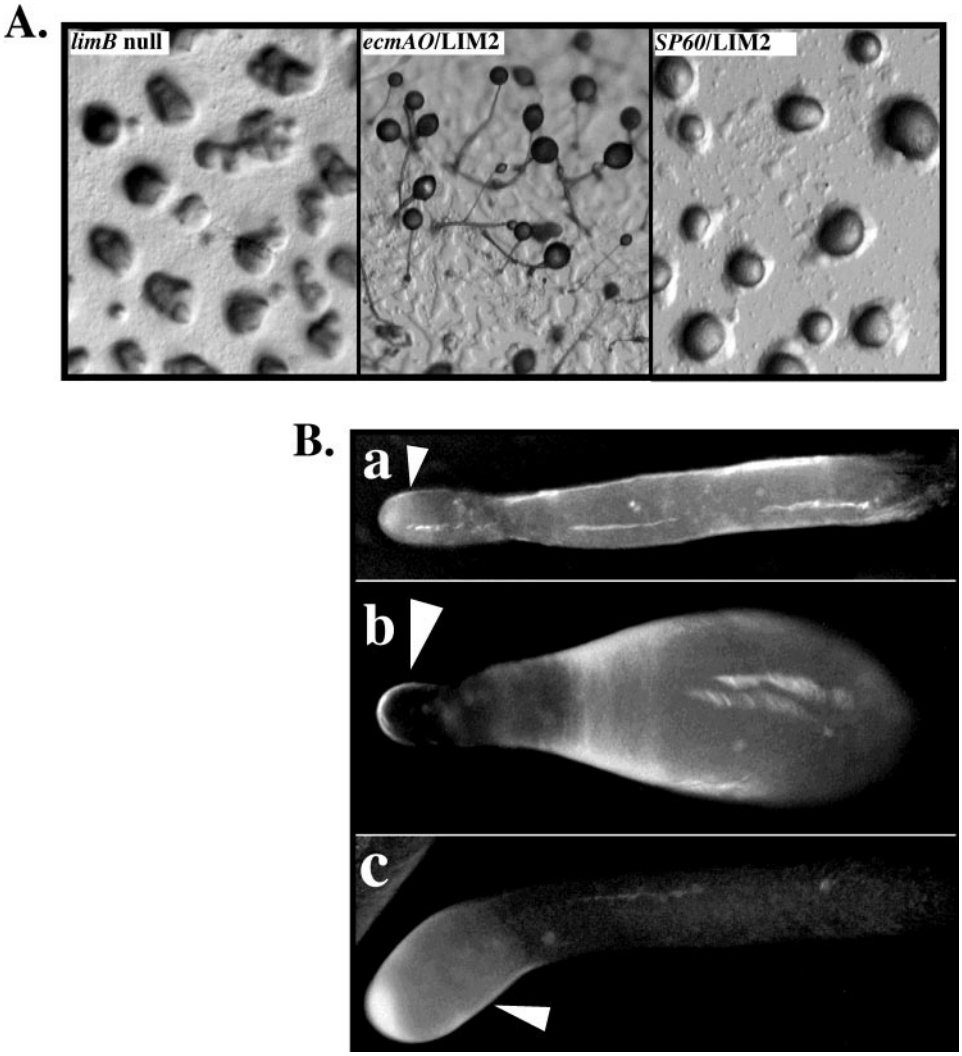

Figure 3. The development and complementation of *limB* cells. (A) The terminal developmental phenotype of the recapitulated *limB* null strain and strains expressing LIM2 from the *ecmAO* prestalk-specific and *SP60/cotC* prespore-specific promoter. Expression of LIM2 in prestalk cells leads to fruiting body production. (B) Cells labeled with the vital fluorescent dye Mitotracker Green were mixed with unlabeled cells and allowed to develop to the slug stage. The white arrowheads indicate the anterior, prestalk region in the anterior of each slug. Panel a shows labeled wild-type KAx-3 mixed 1:3 with unlabeled KAx-3 and indicates uniform staining throughout the slug. Panel b shows the staining pattern of a slug composed of 1:3 labeled *limB* null cells mixed with unlabeled KAx-3. Only the posterior, prespore region contains stained cells. In panel c, one part *limB* null cells expressing *ecmA/LIM2* was mixed with three parts unlabeled KAx-3 cells. The slug has strong staining in the anterior prestalk region, but only faint staining in the prespore region, which may be anterior-like cells.

chemotaxis of *limB* null cells directly, we used DIC microscopy to examine the movement of aggregation-stage cells toward a micropipette emitting the chemoattractant cAMP (see MATERIALS AND METHODS). Time-lapse images of *limB* null cells (Figure 5B) show that the cells are significantly less polarized than wild-type (KAx-3) cells (Figure 5A) and move more slowly without protruding major pseudopodia toward the cAMP source. As demonstrated in Figure 5Bb (a, b, and d), *limB* null cells have numerous microspikes (filapodia), seen as spiny projections from the surface of the cells. In addition, some of the cells (significantly more than wild-type cells) project more than one dominant pseudopod (Figure 5Bb, b and c).

limB null cells also exhibit growth phenotypes. In suspension culture, their growth rate is significantly slower than that of wild-type cells, growing with an average doubling time of 18.5 ± 2 h compared with 10.5 ± 1 h for wild-type cells (our unpublished results). On plastic Petri dishes, the cells are less adherent to the bottom of the dish than wild-type cells and are easily dislodged (our unpublished results). These defects in cell morphology and adherence suggest that *limB* null cells may have an altered cytoskeletal organization. *limB* null cells were not multinucleate under any growth condition as determined by DAPI staining (our unpublished results).

limB Null Cells Exhibit a Defect in Cell Type-specific Gene Expression and the Formation of Cell–Cell Contacts

The developmental pattern of *limB* expression is shown in Figure 6A. *limB* transcripts are first detectable in our RNA blots at 4 h of development, peak at 8–12 h, and then decrease for the remainder of development. On the basis of our observations of growth defects in *limB* null strains, the protein must be expressed in vegetative cells as well, but the level of transcripts must be significantly lower than that observed during aggregation.

To determine whether aggregation and postaggregative gene expression is altered in *limB* null cells, we used RNA blots probed with *csA/gp80* and *LagC*, respectively. Aggregation-stage genes such as *csA/gp80* are induced in response

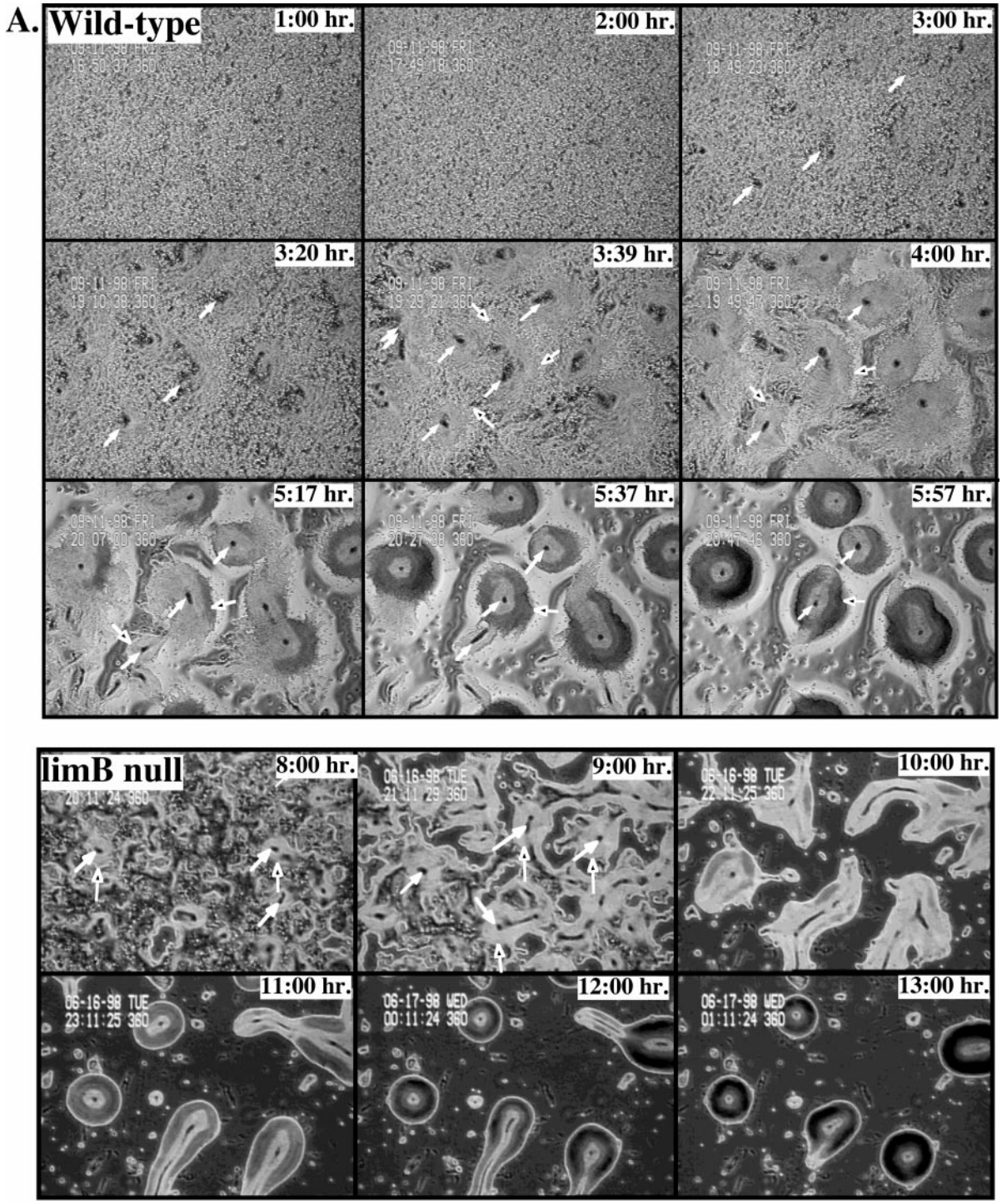

Figure 4. Time-lapse video microscopy of aggregating cells. (A, top panels) Wild-type cells. (A, bottom panels) *limB* null cells. Washed, starved cells were plated as an ~95% confluent monolayer on thin agar, and aggregation was recorded by time-lapse video, phase-contrast microscopy as described previously (Ma *et al.*, 1997; Meili *et al.*, 1999) (see MATERIALS AND METHODS). Some of the aggregation centers are indicated by a solid, white arrow. The outside of aggregation domains is indicated by a solid black arrow. (B) Rotational cell trajectories in *limB* null mounds. A small number of Act15/GFP-tagged *limB* null cells were mixed with unlabeled *limB* null cells and allowed to aggregate. Time-lapse fluorescence movies were collected to assess cell motion. Left, bright-field view of a *limB* null mound. Right, trajectories of fluorescently tagged cells from the same mound. A cell's center of mass is indicated by a square with a gray scale that indicates the flow of time. Lines connecting the squares represent successive positions of the same cell. Time points are separated by 2-min intervals.

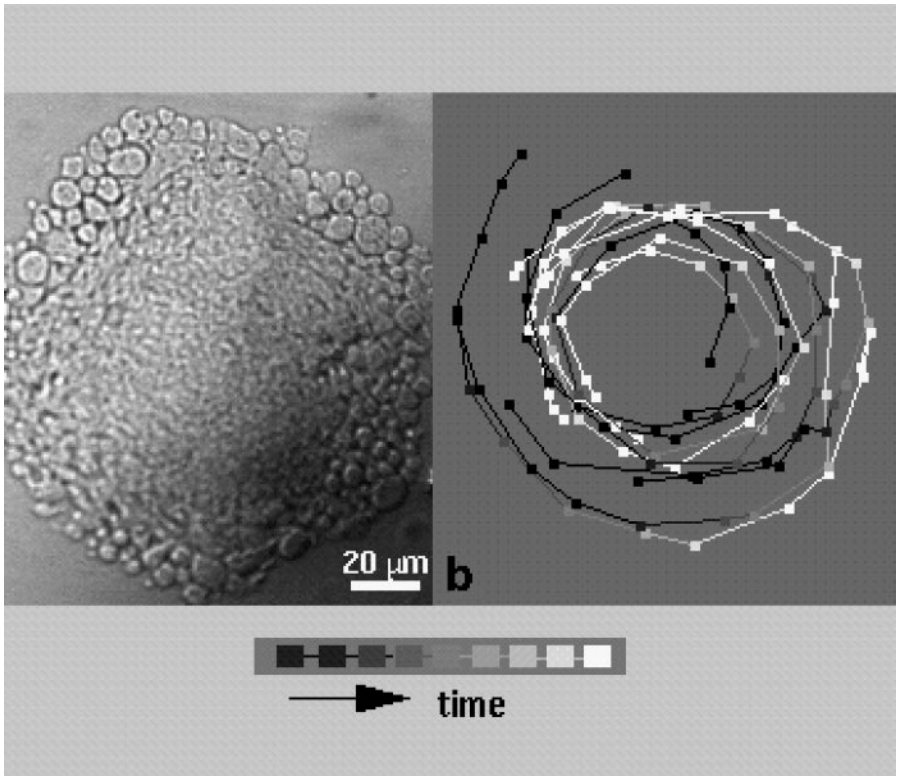

Figure 4 (Continued).

to oscillatory pulses of cAMP via a receptor-mediated, G protein-dependent signaling pathway (Noegel *et al.*, 1985; Mann and Firtel, 1989; Wu *et al.*, 1995). As shown in Figure 6B, *csA* exhibits similar kinetics of induction in wild-type and *limB* cells; however, in the wild-type strain, *csA* expression is down-regulated after 8 h of development in the mound, whereas *csA* expression remains high in *limB* null cells, possibly because of the arrest of the *limB* null cells at the mound stage. Postaggregative genes are induced during late aggregation and mound formation in response to high, continuous levels of cAMP via a receptor-dependent but G protein-independent pathway (Schnitzler *et al.*, 1995). The postaggregative gene *LagC*, a marker for this stage of development, is required for morphogenesis and subsequent cell-type differentiation (Dynes *et al.*, 1994). Induction of *LagC* expression is similar in both *limB* cells and wild-type KAx-3 cells, but *LagC* expression in *limB* null cells remains at a high level, whereas *LagC* expression levels decrease in wild-type organisms as described previously (Dynes *et al.*, 1994).

The lack of down-regulation of *csA* and *LagC* in limB null cells suggests that there may be an absence of cell sorting and subsequent cell-type differentiation. To examine cell-type–specific gene expression, RNA blots were probed for the prestalk-specific genes *ecmA* and *ecmB,* expressed in prestalk (pst) A/O and B cells, respectively, and the prespore-specific marker *SP60/cotC* (Jermyn *et al.*, 1989; Haberstroh and Firtel, 1990; Early *et al.*, 1993). In *limB* cells, the level of *SP60/cotC* gene expression is slightly reduced compared with that of wild-type cells. The kinetics of induction are delayed, consistent with the delay in aggregate formation in this strain (Figure 6B). The prestalk-specific markers, however, exhibit a significantly decreased level and delayed expression, suggesting that *limB* null cells are deficient in prestalk cell differentiation. As expected, *limB* null cells lack the high induction of *ecmB* during later development seen in wild-type organisms, which corresponds to the induction of stalk cell differentiation.

In some mutant strains, defects in cell-type–specific gene expression can be complemented by giving the cells extracellular cAMP, which mimics the normal cAMP signaling of wild-type cells (Dynes *et al.*, 1994; Insall *et al.*, 1994; Soede *et al.*, 1994). As shown in Figure 6C, both *SP60/cotC* and *ecmA* exhibit cAMP-dependent expression; however, RNA levels are reduced significantly in the *limB* null cells as compared with wild-type KAx-3. For *SP60/cotC*, the expression level is also reduced compared with the expression level in *limB* null cells undergoing multicellular development (compare *SP60/cotC* expression in *limB* null and wild-type cells in Figure 6, B and C). Expression of *ecmA* and *SP60/cotC* is cAMP-dependent in both *limB* null and wild-type cells.

Wild-type cells form clumps under the cell culture conditions used to assay cell-type–specific gene expression in suspension, which is due to increased cell–cell adhesion (Mehdy and Firtel, 1985). Wild-type cells form only small clumps after 5 h of treatment with 30 nM pulses of cAMP at moderate speeds (120 rpm) (Figure 7), conditions that mimic the oscillatory pulses of cAMP sensed by the cells during aggregation (Mann and Firtel, 1987; Insall *et al.*, 1994; Soede *et al.*, 1994; Ma *et al.*, 1997); however, wild-type cells form large, tight aggregates if shaking is continued for an additional 3 h, whether or not additional exogenous cAMP is added. In contrast, *limB* null cells do not form clumps under

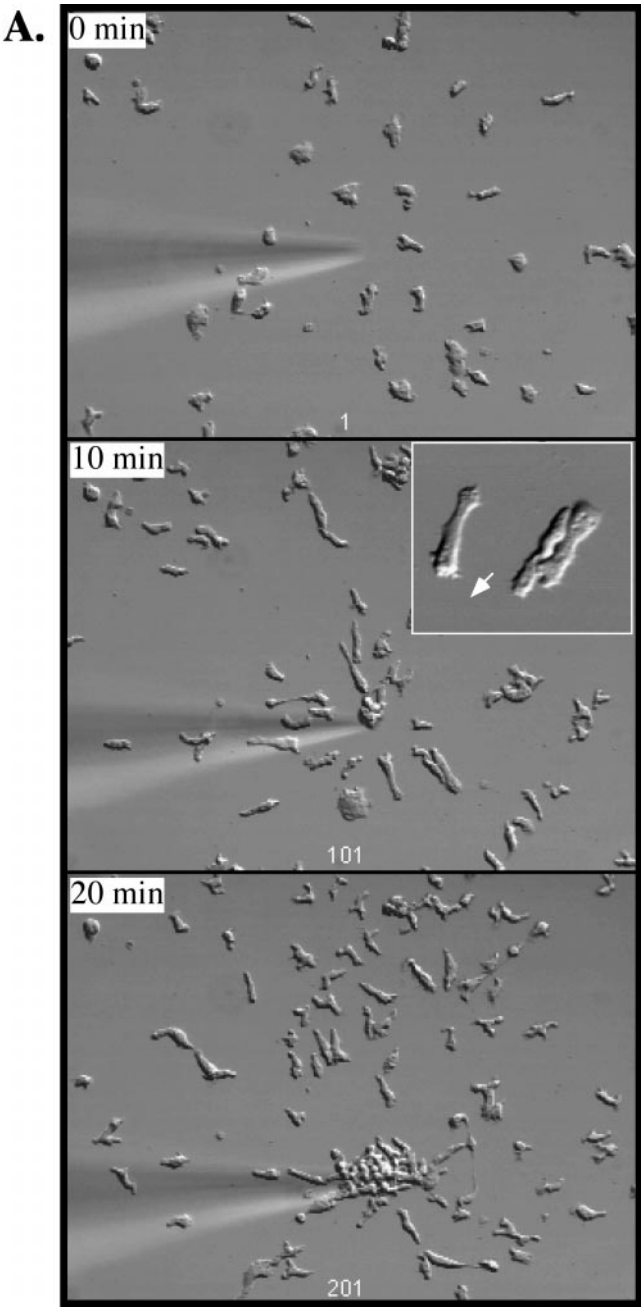

Figure 5. Chemotaxis of cells to a micropipette containing the chemoattractant cAMP. Wild-type cells (A) or *limB* null cells (B) were washed and pulsed with 30 nM cAMP for 5 h to maximize expression of aggregation-stage chemotaxis signaling pathways (Insall *et al.*, 1994; Ma *et al.*, 1997; Meili *et al.*, 1999). Cells were plated on a glass coverslip and allowed to adhere, and a micropipette containing cAMP was inserted (for details see Lee *et al.*, 1999; Meili *et al.*, 1999) (see MATERIALS AND METHODS). Insert in A shows an enlargement of wild-type cells. Ba shows the chemotaxis of *limB* null cells. Bb (a–c) shows an enlargement of three of these cells. Bb (d) shows a DIC image of two cells taken with a 60× objective. Arrows point to filopodia.

any of the conditions tested. Because cell–cell or cell–substratum contacts are required for efficient cell-type–specific gene expression strains (Mehdy and Firtel, 1985; Dynes *et al.*, 1994), these data suggest that the highly reduced prespore- and prestalk-specific gene expression in *limB* null cells may be due to a defect in cell–cell contact formation in the suspension assay. In addition, this effect might indicate a defect in *limB* null cells that could account, in part, for the reduced expression of these genes in *limB* null mounds.

Spatial Patterning of limB Null Cells

To examine whether *limB* null cells were capable of forming the different parts of the developing organism, we tagged *limB* null cells with reporter constructs and examined their ability to sort and form specific structures in chimeric organisms with wild-type strains. *limB* null cells expressing *lacZ* or GFP from the *Act15* promoter, which is expressed in all cells, were mixed with a threefold excess of wild-type cells in the case of *lacZ* and a 10-fold excess in the case of GFP (Figure 8, A and C). Most of the *limB* null cells are found at the base of the mound or surrounding the mound, and relatively few are found in the upper portion of a tight aggregate forming a tip (Figure 8, Aa and Ca), suggesting that most *limB* null cells were excluded from cell sorting in the mound. In slugs, the *limB* null cells are found predominantly as a layer around the outside of the slug or in the posterior (Figure 8, Ab and Cb). Very few *limB* null cells are found within the slug mass, in either the prestalk or prespore domain (Figure 8, Ab and Cb). In fruiting bodies, *limB* null cells are found mostly in the lower cup, in the layer of cells surrounding the spore mass, or at the base of the stalk and basal disk (Figure 8A, c and d). Very few of the *limB* null cells associated with the stalk exhibit normal stalk cell characteristics. No stained spores or spore-like cells are observed. In addition, no *limB* null detergent- and heat-resistant spores are formed when cell viability is tested (<0.02%; our unpublished results). These results suggest that the stained, *limB* null cells in the slugs may be undifferentiated or anterior-like rather than prespore cells.

Because *limB* null cells induce prestalk and prespore cells when allowed to develop on their own, the inability to participate in normal slug structures may be due to their cell movement defects and their localization at the periphery of the developing chimeric aggregate. To address these possibilities, we examined the motion of the *limB* null cells in chimeric aggregates (Figure 8C). *limB* null cells at the mound periphery jiggle actively, but most are unable to enter the aggregate. The few cells that appear to be inside the mound show virtually no motion, although bright-field images of the same mound reveal a rotational flow. Thus, the *limB* null cells, when competing with wild-type cells, exhibit striking defects in motility.

To directly examine the participation of *limB* null cells in the formation of the prestalk and prespore domains, we tagged *limB* null cells with either the prestalk marker *ecmAO/lacZ* or the prespore marker *SP60/lacZ* and allowed them to form chimeras with wild-type cells (Figure 8B). (Note: *ecmAO* is the complete promoter of the *ecmA* gene and is expressed in pstA and pstO cells [Early *et al.*, 1993].) Few *limB* null cells expressing the prespore-specific marker *SP60/lacZ* are found in chimeras. The cells are localized to the posterior of slugs and appear mostly on the outer layer of cells in the slug and mature spore mass (Figure 8B, c and f). *limB* null cells expressing *ecmAO/lacZ*,

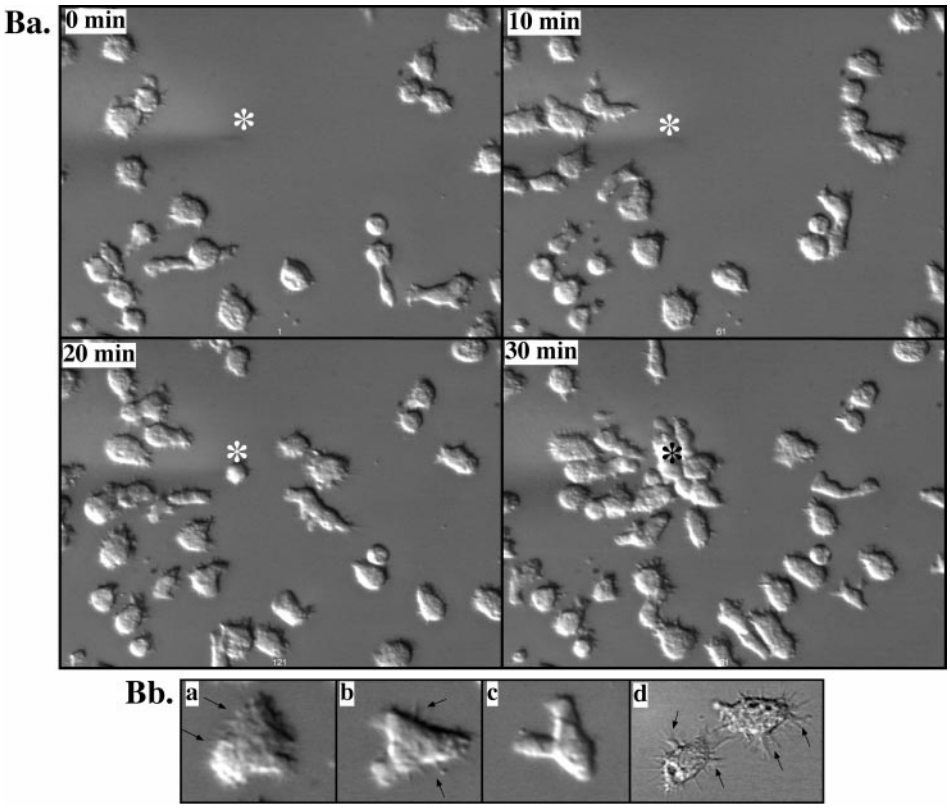

Figure 5 (Continued).

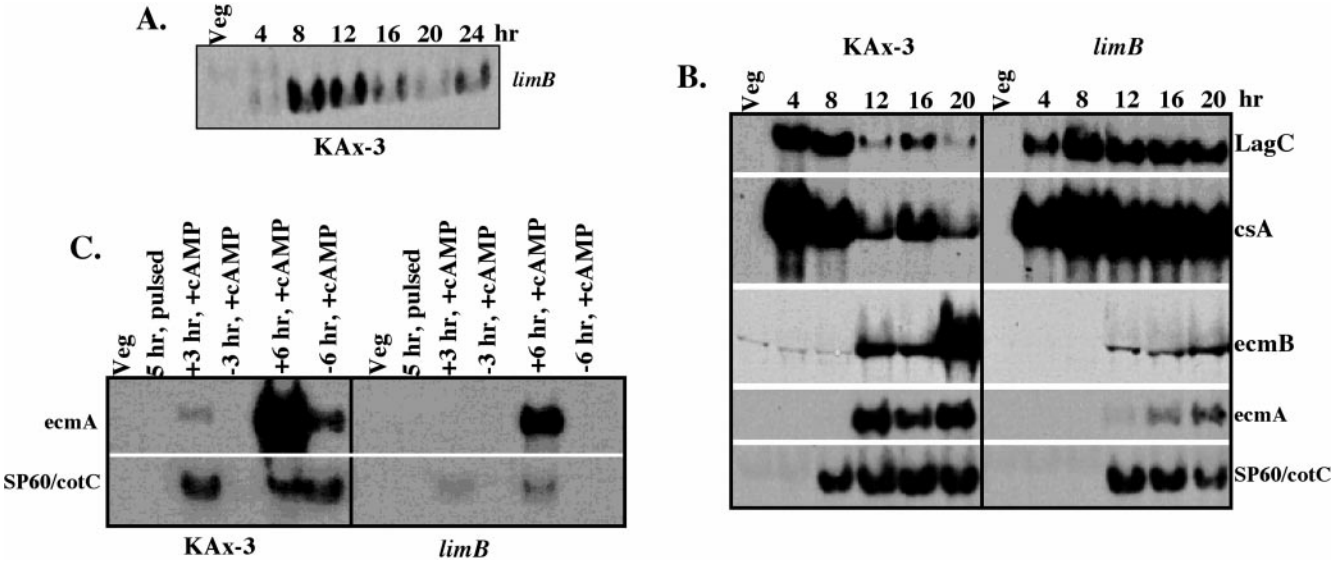

Figure 6. Developmental RNA blots. The number of hours after the beginning of development is written above each lane. In addition, a vegetative cell lysate is included for each strain and blot. (A) Developmental expression of *limB*. The number of hours above each lane is the time from plating. (B) Developmental expression of the cAMP-pulsed induced gene *csA* (encoding the cell adhesion protein csA/gp80), the postaggregative gene *LagC* (required for development past the mound stage), the prestalk genes *ecmA* and *ecmB*, and the prespore gene *SP60/cotC*. (C) Induction of prestalk (*ecmA*) and prespore (*SP60/cotC*) gene expression in suspension culture as previously described (Mehdy and Firtel, 1985; Dynes *et al*., 1994). Washed, log-phase vegetative cells (6×10^5 cells/ml) were pulsed every 6 min with cAMP to a final concentration of 30 nM for 5 h at 120 rpm. Cells were then split and shaken with or without addition of cAMP to 300 μM cAMP for an additional 3 or 6 h, with cAMP supplemented to 100 μM every 3 h. RNA was isolated at the times indicated and analyzed by RNA blot hybridization.

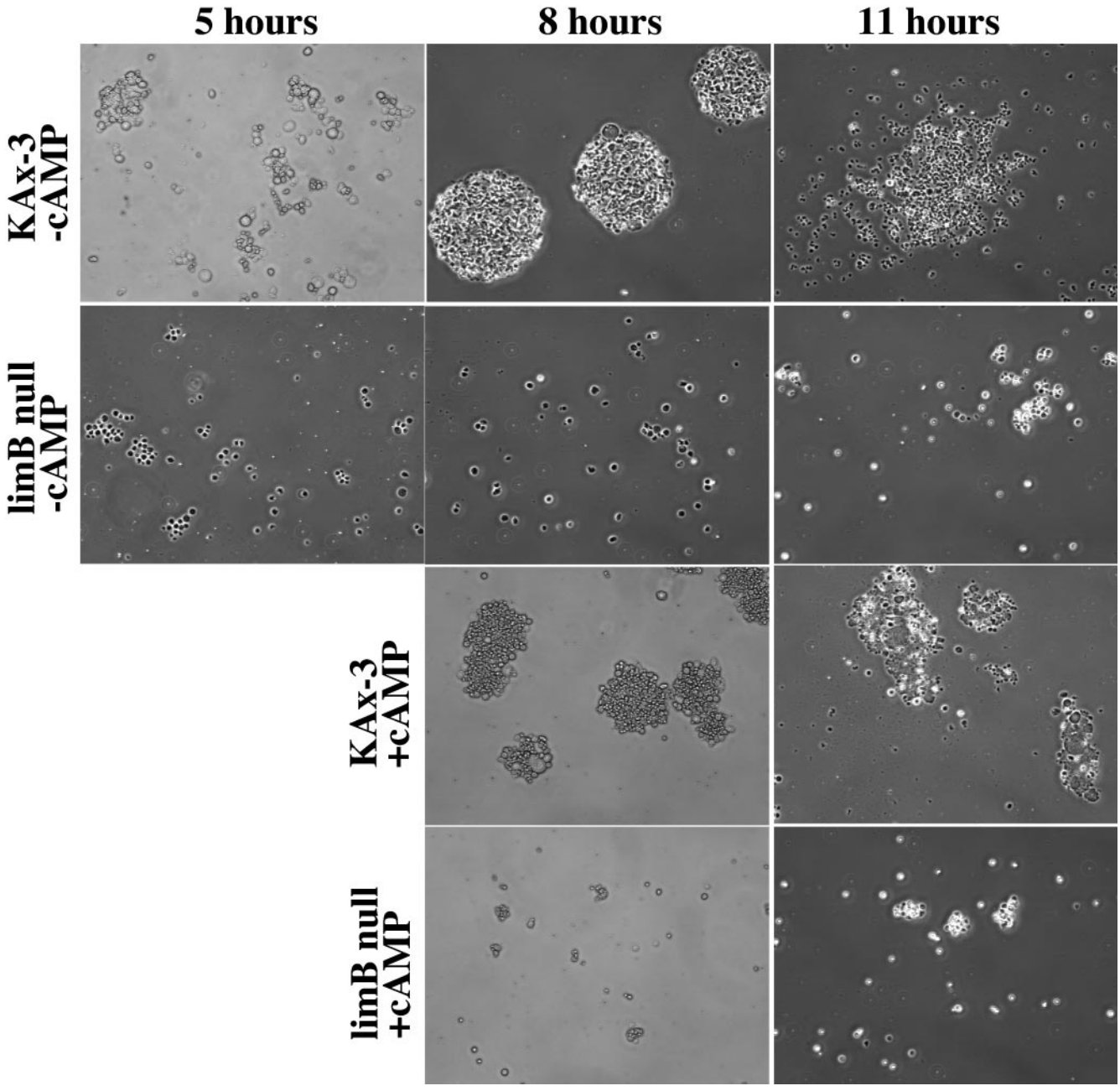

Figure 7. *limB* null cells do not form cell agglomerates in suspension. Wild-type and *limB* null cells were pulsed with 30 nM cAMP in suspension for 5 h and then treated with high, continuous cAMP as described in the legend to Figure 6C and MATERIALS AND METHODS. Aliquots were taken from cell suspension and examined under phase-contrast microscopy. Time points are the same as those in Figure 6C.

which form the pstA and pstO anterior prestalk domains in wild-type strains, are mostly excluded from the anterior prestalk domain in the chimeras and are found mainly at the base of aggregates forming tips (Figure 8Ba), in the posterior of slugs and on the slug's surface (Figure 8Bb), and in the lower cup of sori and on the surface of the stalk (Figure 8B, d and e). Our results are consistent with LIM2 being required for cell sorting within the mound.

Expression of LIM2 under a Prestalk but Not a Prespore Promoter Complements the limB Developmental Phenotype

We have demonstrated that LIM2 function is important for the organization of the actin cytoskeleton and developmentally for chemotaxis, cell sorting, tip formation, and morphogenesis. Tip formation occurs through the sorting of prestalk

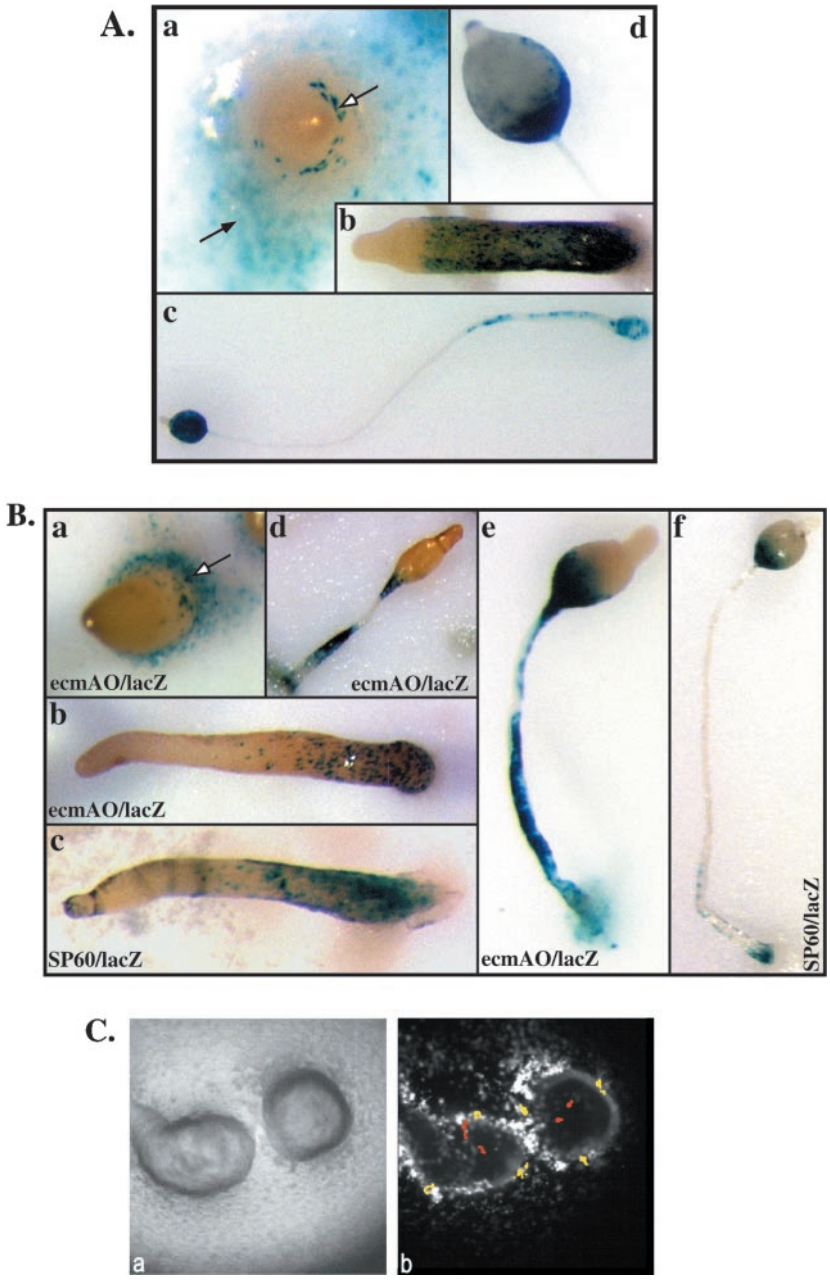

Figure 8. Spatial localization of *limB* null cells in multicellular organisms. (A) One part *limB* null cells expressing *Act15/lacZ* were mixed with three parts KAx-3 cells. Aggregates were stained for β-galactosidase activity at various stages of development. (a) Mound stage. Labeled cells are primarily in the periphery of the mound (see open arrows). A few cells can be seen in the mound. (b) Slug stage. Stained cells are in a surface layer around the posterior 75% of the slug. (c) Fruiting body. Stained cells are found on the surface of the stalk and lower cup. (d) Closeup of the head of a fruiting body (sorus) showing staining of the lower cup or cells surrounding the lower portion of the sorus. (B) *limB* null cells expressing either *ecmAO/lacZ* or *SP60/lacZ* were mixed 1:3 with KAx-3 cells and stained for β-galactosidase activity at various developmental stages. (a) Tipped aggregate, *limB* null *ecmAO/lacZ*:KAx-3. (b) Slug, *limB* null *ecmAO/lacZ*:KAx-3. (c) Slug, *limB* null *SP60/lacZ*:KAx-3. (d) Early culminant, *limB* null *ecmAO/lacZ*:KAx-3. (e) Culminant, *limB* null *ecmAO/lacZ*:KAx-3. (f) Culminant, *limB* null *SP60/lacZ*:KAx-3. (C) One part *limB* null cells expressing Act15/GFP were mixed with 10 parts wild-type cells, and time-lapse movies were captured. (a) Bright-field view of two chimeric mounds. Movies indicate a rotational flow characteristic of wild-type cells of this strain. (b) Fluorescent image of the same mounds. Most of the *limB* null cells are found at the mound periphery, with a much smaller number of mutant cells located inside the mounds. Time-lapse movies of these mounds reveal that the *limB* null cells jiggle largely in place, either at the mound periphery or inside the mound. Cell trajectories are indicated by colored dots, yellow for cells at the periphery and red for cells in the mound interior. Each trajectory is composed of 25 dots representing cell position at 2-min time intervals over a period of 50 min. Because of the defective motion of the *limB* null cells, most of the dots are superimposed, and therefore the trajectories appear as large spots.

Table 1. The terminal phenotype of *limB* null cells expressing each construct

Construct	Intact LIM domains	Comments	Terminal phenotype when expressed in *limB* null cells
1	1–5, no N terminus	Deletes non-LIM N terminus	Full complementation; wild-type development
2	1–4	Deletes non-LIM N terminus and C terminus	Mounds dissociate and reaggregate, eventually forming few slug-like structures
3	2–4	Contains only LIM domains 2–4	No complementation; mound arrest
4	2–5	Deletes N terminus and LIM domain 1	Mounds dissociate and reaggregate, eventually forming few slug-like structures
5	4 and 5	Deletes N terminus and LIM domains 1–3	No complementation; mound arrest
6	None	Deletes LIM domains 1–5 and C terminus	No complementation; mound arrest
7	1 and 2	Deletes LIM domains 3–5 and C terminus	No complementation; mound arrest
8	3–5	Deletes LIM domains 1 and 2	Partial complementation; forms abnormal culminant-like structures
9	1–5	Deletes C terminus	Full complementation; wild-type development
C287S,C290S	1 and 3–5	Contains mutation in LIM domain 2	Partial complementation; forms abnormal slug-like structures
C412S,C415S	1–3 and 5	Contains mutation in LIM domain 4	Partial complementation; forms abnormal slug-like structures

The structure of each construct is as follows: 1) residues 190–550 (end of LIM2); 2) residues 190–436; 3) residues 255–436; 4) residues 255–550; 5) residues 366–550; 6) residues 1–210; 7) residues 1–357; 8) residues 1–210, 273–550; 9) residues 1–518. All N-terminal deletions were expressed in-frame from the Act15 promoter with an ATG translation initiation codon.

cells to the apical region of the mound and subsequent extension of this apical region (Durston and Vork, 1979). To determine whether LIM2 is preferentially required in prestalk or prespore cells for tip formation, we expressed LIM2 under the control of the *SP60/cotC* prespore promoter and the *ecmAO* prestalk promoter. The *limB* developmental phenotype was complemented when it was expressed in prestalk but not prespore cells (Figure 2A), suggesting that LIM2 is required for proper regulation of motility or adhesion for prestalk cell differentiation and/or migration in the mound.

We examined the localization of *limB* null cells expressing LIM2 from the *ecmAO* promoter in chimeric slugs made up of three parts KAx-3 and one part *limB* null cells expressing *ecmAO*/LIM2, which we tagged with Mitotracker Green. In such chimeras, the anterior region of the slug stains brightly, as do individual cells in the posterior prespore region that probably correspond to anterior-like cells (Figure 3Bc), indicating that these cells are fully competent to sort and form the prestalk domains of the organism. In chimeras containing wild-type cells mixed with *limB* null cells labeled with Act/GFP, the *limB* null cells exhibit the same distribution as *limB* null cells tagged with *Act15/lacZ*: staining is restricted to the posterior of developing slugs, leaving the prestalk region at the anterior of the slug unstained (Figure 3Ba). As expected, in a chimera containing ~7% wild-type cells labeled with Mitotracker Green mixed with 93% unlabeled wild-type cells, the fluorescent cells are evenly distributed throughout the organism (Figure 3Ba).

Mutational Analysis of LIM Domain Function

To determine the role of individual LIM domains in the function of LIM2, a series of deletion mutations were constructed and expressed in wild-type and *limB* null cells from the *Act15* promoter (Table 1). KAx-3 cells expressing these constructs under *Act15* develop normally (our unpublished results). Overexpression of a LIM2 construct containing all of the LIM domains but lacking the N-terminal domain (LIM2–1) or one lacking the highly basic terminal 31 C-terminal amino acids (constructs LIM2–1 and LIM2–9, respectively) complements the *limB* null phenotype (see Table 1 for summary). Constructs LIM2–5, -6, and -7, which delete LIM domains 4 and 5, 1–5, or 1 and 2, respectively, fail to complement the mound-arrest phenotype, and the phenotypes are indistinguishable from those of the *limB* null strain. *limB* null strains expressing constructs LIM2–2 and LIM2–4 form mounds that subsequently dissociate into ring-like structures that reform mounds. This process continues for *limB* null cells overexpressing LIM2–2 over the ~36 h for which the cells were followed, whereas cells expressing LIM2–4 arrest at the mound stage after the first reassociation. The LIM2–8, which contains LIM domains 3 through 5, partially complements the *limB* null mound-arrest phenotype. These cells aggregate and form tight mounds by 11 h. Some of the mounds form normal-looking slugs by 16 h; however, these eventually develop into abnormally shaped structures resembling slugs supported by thin stalk-like structures.

To examine the importance of the second LIM domain, we introduced point mutations in which the conserved Cys at positions 287 and 290 were mutated to Ser (strain LIM2^{C287S,C290S}), thereby abolishing one of the two Zn^{2+} coordination sites in the LIM domain. A similar mutation was made in the fourth LIM domain (strain LIM2^{C412S,C415S}). Expression of these constructs in KAx-3 had no effect on development, and both constructs partially complement the

limB background. The *limB* null strain expressing LIM2^{C287S,C290S} eventually differentiates into abnormal fruiting bodies, whereas the *limB* null strain expressing LIM2^{C412S,C415S} forms terminal structures with oddly shaped sori on top of thick, tube-like stalks. LIM2^{C412S,C415S}-expressing *limB* cells halt development at the slug stage (our unpublished results). Using phalloidin staining, we also examined whether the LIM2 mutant proteins alter the defects in the actin cytoskeleton exhibited by *limB* null cells. We observed a direct correlation between the ability of a LIM2 construct to complement the *limB* null developmental phenotype and the ability to restore the shape of the cell and the structure of the actin cytoskeleton (our unpublished results).

DISCUSSION

LimB Is Required for Tip Formation and Subsequent Morphogenesis

Understanding the pathways that control cell movement during morphogenesis is the key to understanding pattern formation and multicellular development. To investigate these processes, we undertook a screen for genes required for morphogenesis in *Dictyostelium* by identifying mutant strains that were unable to form a tipped aggregate. Such strains would be expected to have a defect in the ability of cells to sort to the apical tip and/or a defect in cell-type–specific gene expression. One of the genes identified in this screen is *limB*, which encodes the LIM domain-containing protein LIM2 and is required for proper morphogenesis. *limB* is one of several genes identified in this screen that, not unexpectedly, is required for the proper organization of the actin cytoskeleton, cell shape, and chemotaxis. *limB* null cells have numerous F-actin-enriched microspikes and adhere poorly to a substratum such as a plastic Petri dish, possibly because they are unable to flatten and spread on the surface. In addition, when placed in a cAMP chemoattractant gradient, these cells are not polarized with respect to cell shape (they are not elongated), and the subcellular localization of actin, which is preferentially found at the leading edge and in the posterior of wild-type chemotaxing cells. These cells do not produce defined pseudopodia in the direction of the chemoattractant and move very slowly compared with wild-type cells. Analysis using GFP–coronin, which binds to F-actin and is used to localize F-actin in vivo (Westphal *et al.*, 1997), demonstrates that GFP–coronin localizes to the edge of the cell in the direction of the cAMP source; however, this response is weak. and the region of the cell that shows this localization is not always aligned with the cAMP gradient or aggregation streams, as it is in wild-type cells. This finding is consistent with the inability of these cells to polarize. Aggregation is delayed compared with wild-type cells and is somewhat "inefficient" in that a variable fraction of cells do not enter the mounds, presumably because of the chemotaxis defects. Interestingly, LIM2 is associated with the cortex of the cell but does not colocalize with F-actin or in regions enriched in myosin II in a polarized cell. A previously discovered *Dictyostelium* LIM domain-containing protein, DdLim1, which is quite distinct from LIM2 in structure and has only a single LIM domain, is also required for proper reorganization of the actin cytoskeleton during lamellipodia formation (Prassler *et al.*, 1998). Like *limB*, *DdLim1* expression is induced during aggregation. Whether the DdLim1 and LIM2 function in the same pathway is not known.

Morphogenesis in *Dictyostelium* involves the differential sorting of prestalk and prespore cells. In wild-type strains, prestalk cells, which are initially found toward the outside and base of the developing mound, sort to the apical region of the mound via a mechanism involving directional movement through the 3-D mass of cells (Siegert and Weijer, 1997; Dormann *et al.*, 1998; Aubry and Firtel, 1999; Clow and McNally, 1999). Evidence indicates that this sorting involves chemotaxis toward cAMP. A first finger forms from an extension of the tip upward, which then falls over onto the substratum, forming a migrating slug or pseudoplasmodium. Disruption of *limB* results in cells that are unable to form a tip, suggesting that *limB* is required for the regulation of the actin cytoskeleton during this process and/or adhesion. Our observation that the expression of LIM2 under the prestalk-specific promoter rescues development of *limB* null cells is consistent with a model whereby *limB* is required for the proper sorting of prestalk cells to form a tip in the developing mound. We suggest that LIM2 is required for proper cell movement during this process.

Previous studies have demonstrated that strains in which the genes encoding components of the cytoskeleton, conventional myosin (myosin II) or myosin regulatory light chain (mlcR), have been disrupted are also unable to form a tip (De Lozanne and Spudich, 1987; Knecht and Loomis, 1987; Chen *et al.*, 1994). As with *limB* null cells, these strains exhibit chemotaxis defects, which include an inability to properly retract the posterior of the cell and a loss or reduction of cortical tension (Wessels *et al.*, 1988; Pasternak *et al.*, 1989; R. Koehl and J. McNally, unpublished data). The defects in rear retraction and cortical tension found in myosin II mutants may prevent cells from moving through a multicellular mass (Doolittle *et al.*, 1995; Shelden and Knecht, 1995; Clow and McNally, 1999) and may preclude cell sorting and tip formation (Traynor *et al.*, 1994; Clow and McNally, 1999). These sorting defects are likely to result in myosin II mutant cells being excluded from chimeric mounds containing wild-type cells (Knecht and Shelden, 1995).

We demonstrate that the *limB* null cells have very abnormal movement, particularly when mixed with wild-type cells. In chimeric mounds, *limB* null cells, like myosin II mutants, are found predominantly at the periphery, where they jiggle and appear unable to penetrate the mound. The few that manage to enter are found mostly at the mound base where they also jiggle in place, whereas the wild-type cells in the same mound exhibit their characteristic rotational flow. As seen in isolated cells or within mounds composed entirely of mutant cells, migrating *limB* null cells are not polarized and form multiple pseudopodia. Time-lapse video microscopy of *limB* null cells in a cAMP gradient reveals little extension of pseudopodia in the direction of the chemoattractant source. Although it is possible that this may be due in part to an inability of the cells to form a strong attachment to the substratum, it is probable that this defect also involves the inability to properly organize the actin cytoskeleton. We think that this defect in actin reorganization leads to the observed developmental phenotypes, in particular the failure to form a tip.

Tip formation and cell patterning are thought to arise from differential movement of prestalk cells through the cell

mass to the top of the mound (Durston and Vork, 1979; Clow and McNally, 1999). To test whether the failure to form a tip in *limB* null mounds arises from defective prestalk cell movement, we expressed LIM2 under the control of a prestalk promoter (ecmAO), which fully rescued the *limB* null mound-arrest developmental phenotype. The complementary experiment with LIM2 expression under the control of a prespore promoter failed to rescue. These studies mirror the results for a myosin mutant, the *mlcR* null strain. Expression of the mlcR from the *ecmAO* prestalk but not a prespore promoter in *mlcR* null cells complements the morphogenetic defects of the null strain (Chen *et al.*, 1998). Our data therefore suggest that the motile defects in the *limB* null cells are especially detrimental to prestalk cell motility and the ability of these cells to sort to form the apical tip. Prestalk cells must segregate from prespore cells, presumably via differential chemotaxis (Durston and Vork, 1979; Clow and McNally, 1999). This process requires that the prestalk cells become interposed with and move around surrounding prespore cells within a 3-D mass and respond appropriately to an attractive chemotactic signal. As we have demonstrated, both motile capabilities are defective in the *limB* null cells, which have difficulty penetrating wild-type mounds and exhibit aberrant chemotaxis. We think that these motile defects in the prestalk cells are likely to underlie the failure to form a tip.

limB Null Cells Exhibit Defects in Cell Adhesion

Differential cell adhesion is also thought to play a role in cell sorting of prestalk and prespore cells and postaggregative development in *Dictyostelium* (Sternfeld, 1979; Levine *et al.*, 1997; Siu *et al.*, 1997; Ginger *et al.*, 1998; Nicol *et al.*, 1999). Prespore cells exhibit preferential adhesion to other prespore cells compared with their interactions with prestalk cells (Lam *et al.*, 1981). *dtfA* null cells, which lack a cellular adhesion protein, exhibit a mound-arrest phenotype similar to that of *limB* (Ginger *et al.*, 1998). Interestingly, *limB* null cells are defective in the ability to form large cell aggregates in suspension culture, which could be due to a defect in cell adhesion or a physical inability to form contacts because of the abnormal shape of *limB* null cells. In addition, *limB* null cells have difficulty in entering and move poorly within wild-type aggregates. These results suggest a defect in cell–cell adhesion or a reduction in the ability to form cell–cell contacts, possibly because of the abnormal structure of *limB* null cells, which may prevent close cell–cell associations. The aggregation-stage cell adhesion molecule contact site A (csA or gp80) (Gerisch, 1968; Harloff *et al.*, 1989; Kamboj *et al.*, 1990; Siu *et al.*, 1997) is expressed in *limB* null cells. *LagC*, which encodes a protein containing a single transmembrane domain with a large extracellular domain and a short intracellular domain (Dynes *et al.*, 1994), is required for proper morphogenesis and normal induction of postaggregative and cell-type–specific genes. It functions nonautonomously in these pathways and is proposed to be involved in cell–cell signaling. In addition, LagC protein is identical to gp150, which has been proposed to be a cell adhesion molecule required for multicellular development (Gao *et al.*, 1992; C.-H. Siu, personal communication). As with csA, LagC is properly induced in *limB* null cells, indicating that the inability of these cells to form large conglomerates or aggregates is not due to the inability to express either of these cell adhesion molecules. It is possible that some of the *limB* null phenotypes are due to an inability of the cells to express another cell adhesion molecule. Alternatively, the inability to form cell aggregates may be due to the abnormal structure of *limB* null cells, which may not allow normal cell–cell contacts to occur. We think that the morphogenetic defects are not due to the observed reduction in cell-type–specific gene expression and that the reduced prestalk and prespore gene expression results from cells arresting at the mound stage. This developmental arrest probably also accounts for our observations that *csA* and *LagC* expression does not drop after mound formation, as occurs in wild-type strains.

Our studies have identified a new gene that is required for cell movement and proper organization of the actin cytoskeleton and is essential for morphogenesis. Although the aggregation defects of *limB* null cells are very discernable, lack of LIM2 expression does not result in cells that are unable to aggregate. We believe that aggregation, in which the initial aggregate is formed, is more forgiving than the sorting of cells within a 3-D structure and subsequent morphogenesis. During aggregation, cells must be able to move on a 2-D surface without having to move through a tight cell mass. Cell sorting, on the other hand, requires the movement of cells through this mass, in which they must be able to extend pseudopodia and move between cells. In mutant strains such as those affecting myosin II function or *limB* null cells, the terminal developmental phenotype that is observed is the inability of cells to sort within the mound. We expect that the same signaling pathways and cytoskeletal reorganizations are required for chemotaxis and morphogenesis: aggregation can occur even in strains in which the reorganization of cytoskeleton in response to chemoattractants is not normal, whereas morphogenesis cannot proceed. It is likely that similar mechanisms are required for movement of cells in metazoan organisms and that the general mechanisms being elucidated in *Dictyostelium* are applicable to other organisms.

ACKNOWLEDGMENTS

We thank members of the Firtel lab for helpful suggestions. The work was supported by a United States Public Health Service grant to R.A.F.

REFERENCES

Ahlgren, U., Pfaff, S., Jessell, T., Edlund, T., and Edlund, H. (1997). Independent requirement for ISL1 in formation of pancreatic mesenchyme and islet cells. Nature *385*, 257–260.

Aubry, L., and Firtel, R.A. (1999). Integration of signaling networks that regulate *Dictyostelium* differentiation. Annu. Rev. Cell Dev. Biol. *15*, 469–517.

Awasthi, V., Doolittle, K.W., Parulkar, G., and McNally, J.G. (1994). Cell tracking using a distributed algorithm for 3D-image segmentation. Bioimaging *1*, 98–112.

Brown, M., Perotta, J., and Turner, C. (1996). Identification of LIM3 as the principal determinant of Paxillin focal adhesion localization and characterization of a novel motif on paxillin directing vinculin and focal adhesion kinase binding. J. Cell Biol. *135*, 1109–1123.

Chen, P.X., Ostrow, B.D., Tafuri, S.R., and Chisholm, R.L. (1994). Targeted disruption of the *Dictyostelium* RMLC gene produces cells

defective in cytokinesis and development. J. Cell Biol. *127*, 1933–1944.

Chen, T.L., Wolf, W.A., and Chisholm, R.L. (1998). Cell-type-specific rescue of myosin function during *Dictyostelium* development defines two distinct cell movements required for culmination. Development *125*, 3895–3903.

Chung, C.Y., and Firtel, R.A. (1999). A p21-activated protein kinase, PAKa, is required for cytokinesis and the regulation of the cytoskeleton in *Dictyostelium* cells during chemotaxis. J. Cell Biol. *147*, 559–575.

Clow, P.A., and McNally, J.G. (1999). *In vivo* observations of myosin II dynamics support a role in rear retraction. Mol. Biol. Cell *10*, 1309–1323.

Conchello, J.A., and McNally, J.G. (1996). Fast regularization technique for expectation maximization algorithm for optical sectioning microscopy. In: IS&T/SPIE Symposium on Electronic Imaging: Science and Technology, *v*ol. 265, San Jose, CA, 199–208.

De Lozanne, A., and Spudich, J.A. (1987). Disruption of the *Dictyostelium* myosin heavy chain gene by homologous recombination. Science *236*, 1086–1091.

Doolittle, K.W., Reddy, I., and McNally, J.G. (1995). 3D analysis of cell movement during normal and myosin-II-null cell morphogenesis in *Dictyostelium*. Dev. Biol. *167*, 118–129.

Dormann, D., Vasiev, B., and Weijer, C.J. (1998). Propagating waves control *Dictyostelium discoideum* morphogenesis. Biophys. Chem. *72*, 21–35.

Durston, A.J., and Vork, F. (1979). A cinamatographical study of the development of vitally stained *Dictyostelium discoideum*. J. Cell Sci. *36*, 261–279.

Dynes, J.L., Clark, A.M., Shaulsky, G., Kuspa, A., Loomis, W.F., and Firtel, R.A. (1994). LagC is required for cell-cell interactions that are essential for cell-type differentiation in *Dictyostelium*. Genes Dev. *8*, 948–958.

Early, A., Abe, T., and Williams, J. (1995). Evidence for positional differentiation of prestalk cells and for a morphogenetic gradient in *Dictyostelium*. Cell *83*, 91–99.

Early, A.E., Gaskell, M.J., Traynor, D., and Williams, J.G. (1993). Two distinct populations of prestalk cells within the tip of the migratory *Dictyostelium* slug with differing fates at culmination. Development *118*, 353–362.

Edwards, D.C., Sanders, L.C., Bokoch G.M., and Gill, G.N. (1999). Activation of LIM-kinase by Pak1 couples Rac/Cdc42 GTPase signaling to actin cytoskeletal dynamics. Nat. Cell Biol. *1*, 253–259.

Freyd, G., Kim, S., and Horvitz, H. (1990). Novel cysteine-rich motif and homeodomain in the product of the *Caenorhabditis elegans* cell lineage gene lin-11. Nature *344*, 876–879.

Gao, E.N., Shier, P., and Siu, C.H. Siu. (1992). Purification and partial characterization of a cell adhesion molecule (gp150) involved in postaggregation stage cell-cell binding in *Dictyostelium discoideum*. J. Biol. Chem. *267*, 9409–9415.

Gerisch, G. (1968). Cell aggregation and differentiation in *Dictyostelium.* In: Current Topics in Developmental Biology, ed. A.A. Moscona and A. Monroy, New York: Academic Press, 157–197.

Gerisch, G., Albrecht, R., Heizer, C., Hodgkinson, S., and Maniak, M. (1995). Chemoattractant-controlled accumulation of coronin at the leading edge of *Dictyostelium* cells monitored using green fluorescent protein-coronin fusion protein. Curr. Biol. *5*, 1280–1285.

Ginger, R.S., Drury, L., Baader, C., Zhukovskaya, N.V., and Williams, J.G. (1998). A novel *Dictyostelium* cell surface protein important for both sell adhesion and cell sorting. Development. *125*, 3343–3352.

Haberstroh, L., and Firtel, R.A. (1990). A spatial gradient of expression of a cAMP-regulated prespore cell type-specific gene in *Dictyostelium*. Genes Dev. *4*, 596–612.

Harloff, C., Gerisch, G., and Noegel, A.A. (1989). Selective elimination of the contact site A protein of *Dictyostelium discoideum* by gene disruption. Genes Dev. *3*, 2011–2019.

Hughes, J.E., Podgorski, G.J., and Welker, D.L. (1992). Selection of *Dictyostelium discoideum* transformants and analysis of vector maintenance using live bacteria resistant to G418. Plasmid *28*, 46–60.

Inoue, A., Takahashi, M., Hatta, K., Hotta, Y., and Okamoto, H. (1994). Developmental regulation of islet-1 mRNA expression during neuronal differentiation in embryonic zebrafish. Dev. Dyn. *199*, 1–11.

Insall, R.H., Soede, R.D.M., Schaap, P., and Devreotes, P.N. (1994). Two cAMP receptors activate common signaling pathways in *Dictyostelium*. Mol. Biol. Cell *5*, 703–711.

Jermyn, K.A., Duffy, K.T., and Williams, J.G. (1989). A new anatomy of the prestalk zone in *Dictyostelium*. Nature *340*, 144–146.

Kamboj, R.K., Lam, T.Y., and Siu, C.H. (1990). Regulation of slug size by the cell adhesion molecule gp80 in *Dictyostelium discoideum*. Cell Regul. *1*, 715–729.

Karlsson, O., Thor, S., Norber, T., Ohlsson, H., and Edlund, E. (1990). Insulin gene enhancer binding protein Isl-1 is a member of a novel class of proteins containing both a homeo- and a Cys-His domain. Nature *344*, 879–882.

Kellerman, K.A., and McNally, J.G. (1999). Mound cell movement and morphogenesis in *Dictyostelium*. Dev. Biol. *208*, 416–429.

Knecht, D.A., and Loomis, W.F. (1987). Antisense RNA inactivation of myosin heavy chain gene expression in *Dictyostelium discoideum*. Science *236*, 1081–1085.

Knecht, D.A., and Shelden, E. (1995). Three-dimensional localization of wild-type and myosin II mutant cells during morphogenesis of *Dictyostelium*. Dev. Biol. *170*, 434–444.

Kuspa, A., and Loomis, W.F. (1992). Tagging developmental genes in *Dictyostelium* by restriction enzyme-mediated integration of plasmid DNA. Proc. Natl. Acad. Sci. USA *89*, 8803–8807.

Lam, T.Y., Pickering, G., Geltosky, J., and Siu, C.H. (1981). Differential cell cohesiveness expressed by prespore and prestalk cells of *Dictyostelium discoideum*. Differentiation *20*, 22–28.

Lee, S., Parent, C.A., Insall, R., and Firtel, ,R.A. (1999). A novel Ras interacting protein required for chemotaxis and cyclic adenosine monophosphate signal relay in *Dictyostelium*. Mol. Biol. Cell *10*, 2829–2845.

Levine, H., Tsimring, L., and Kessler, D. (1997). Computational modeling of mound development in *Dictyostelium*. Physica D. *106*, 375–388.

Loomis, W.F. (1982). The Development of *Dictyostelium discoideum*. New York: Academic Press.

Ma, H., Gamper, M., Parent, C., and Firtel, R.A. (1997). The *Dictyostelium* MAP kinase kinase DdMEK1 regulates chemotaxis and is essential for chemoattractant-mediated activation of guanylyl cyclase. EMBO J. *16*, 4317–4332.

Mann, S.K., and Firtel, R.A. (1989). Two-phase regulatory pathway controls cAMP receptor-mediated expression of early genes in *Dictyostelium*. Proc. Natl. Acad. Sci. USA *86*, 1924–1928.

Mann, S.K.O., *et al*. (1994). Cell biological, molecular, genetic, and biochemical methods to examine *Dictyostelium.* In: Cell Biology: A Laboratory Handbook, ed. J.E. Celis, San Diego: Academic Press, 412–451.

Mann, S.K.O., and Firtel, R.A. (1987). Cyclic AMP regulation of early gene expression in *Dictyostelium discoideum*: mediation via the cell surface cyclic AMP receptor. Mol. Cell. Biol. *7*, 458–469.

Mee, J.D., Tortolo, D.M., and Coukell, M.B. (1986). Chemotaxis-associated properties of separated prestalk and prespore cells of *Dictyostelium discoideum*. Biochem. Cell Biol. *64*, 722–732.

Mehdy, M.C., and Firtel, R.A. (1985). A secreted factor and cyclic AMP jointly regulate cell-type-specific gene expression in *Dictyostelium discoideum*. Mol. Cell. Biol. *5*, 705–713.

Meili, R., Ellsworth, C., Lee, S., Reddy, T.B.K., Ma, H., and Firtel, R.A. (1999). Chemoattractant-mediated transient activation and membrane localization of Akt/PKB is required for efficient chemotaxis to cAMP in *Dictyostelium*. EMBO J. *18*, 2092–2105.

Nellen, W., Datta, S., Reymond, C., Sivertsen, A., Mann, S., Crowley, T., and Firtel, R.A. (1987). Molecular biology in *Dictyostelium*: tools and applications. In: Methods in Cell Biology, vol. 28, ed. J.A. Spudich, Orlando, FL: Academic Press, 67–100.

Nicol, A., Rappel, W.-J., Levine, H., and Loomis, W.F. (1999). Cell-sorting in aggregates of *Dictyostelium discoideum*. J. Cell Sci. *112*, in press.

Noegel, A., Harloff, C., Hirth, P., Markl, R., Modersitzki, M., Stadler, J., Weinhart, U., Westphal, M., and Gerisch, G. (1985). Probing an adhesion mutant of *Dictyostelium discoideum* with cDNA clones and monoclonal antibodies indicates a specific defect in the contact site A glycoprotein. EMBO J. *4*, 3805–3810.

Parent, C.A., Blacklock, B.J., Froehlich, W.M., Murphy, D.B., and Devreotes, P.N. (1998). G protein signaling events are activated at the leading edge of chemotactic cells. Cell *95*, 81–91.

Pasternak, C., Spudich, J.A., and Elson, E.L. (1989). Capping of surface receptors and concomitant cortical tension are generated by conventional myosin. Nature *341*, 549–551.

Pfaff, S., Mendelsohn, M., Stewart, C., Edlund, T., and Jessell, T. (1996). Requirement of LIM homeobox gene Isl1 in motor neuron generation reveals a motor neuron-dependent step in interneuron differentiation. Cell *84*, 309–320.

Prassler, J., Murr, A., Stocker, S., Faix, J., Murphy, J., and Marriott, G. (1998). DdLIM is a cytoskeleton-associated protein involved in the protrusion of lamellipodia in *Dictyostelium*. Mol. Biol. Cell *9*, 545–559.

Preza, C., Miller, M.I., Thomas, L.J., and McNally, J.G. (1992). Regularized linear method for reconstruction of three-dimensional microscopic objects from optical sections. J. Opt. Soc. Am. *9*, 219–228.

Sadler, I., Crawford, A., Michelsen, J., and Beckerle, M. (1992). Zyxin and cCRP: two interactive LIM domain proteins associated with the cytoskeleton. J. Cell Biol. *119*, 1573–1587.

Schmeichel, K., and Beckerle, M. (1994). The LIM domain is a modular protein-binding interface. Cell *79*, 211–219.

Schnitzler, G.R., Briscoe, C., Brown, J.M., and Firtel, R.A. (1995). Serpentine cAMP receptors may act through a G protein-independent pathway to induce postaggregative development in *Dictyostelium*. Cell *81*, 737–745.

Shelden, E., and Knecht, D.A. (1995). Mutants lacking myosin II cannot resist forces generated during multicellular morphogenesis. J. Cell Sci. *108*, 1105–1115.

Siegert, F., and Weijer, C. (1997). Control of cell movement during multicellular morphogenesis. In: *Dictyostelium*: A Model System for Cell and Developmental Biology, ed. Y. Maeda, K. Inouye, and I. Takeuchi, Tokyo: Universal Academy Press, 425–436.

Siegert, F., and Weijer, C.J. (1995). Spiral and concentric waves organize multicellular *Dictyostelium* mounds. Curr. Biol. *5*, 937–943.

Siu, C.H., Harris, T.J.C., Wong, E.F.S., Yang, C., Sesaki, H., and Wang, J. (1997). Cell adhesion molecules in *Dictyostelium.* In: *Dictyostelium*: A Model System for Cell and Developmental Biology, ed. Y. Maeda, K. Inouye, and I. Takeuchi, Tokyo: Universal Academy Press, 111–121.

Soede, R.D.M., Insall, R.H., Devreotes, P.N., and Schaap, P. (1994). Extracellular cAMP can restore development in *Dictyostelium* cells lacking one, but not two subtypes of early cAMP receptors (cARs). Evidence for involvement of cAR1 in aggregative gene expression. Development *120*, 1997–2002.

Spudich, J.A., Finer, J., Simmons, B., Ruppel, K., Patterson, B., and Uyeda, T. (1995). Myosin structure and function. Cold Spring Harb. Symp. Quant. Biol. *60*, 783–791.

Sternfeld, J. (1979). Evidence for differential cellular adhesion as the mechanism of sorting-out of various cellular slime mold species. J. Embryol. Exp. Morphol. *53*, 163–178.

Taira, M., Evrard, J.-L., Steinmetz, A., and Dawid, I.B. (1995). Classification of LIM proteins. Trends Genet. *11*, 431–432.

Thor, S., Ericson, J., Brannstrom, T., and Edlund, T. (1991). The homeodomain LIM protein Isl-1 is expressed in subsets of neurons and endocrine cells in the adult rat. Neuron *7*, 881–889.

Traynor, D., Kessin, R.H., and Williams, J.G. (1992). Chemotactic sorting to cAMP in the multicellular stages of *Dictyostelium* development. Proc. Natl. Acad. Sci. USA *89*, 8303–8307.

Traynor, D., Tasaka, M., Takeuchi, I., and Williams, J. (1994). Aberrant pattern formation in myosin heavy chain mutants of *Dictyostelium*. Development *120*, 591–601.

Turner, C., and Miller, J. (1994). Primary sequence of paxillin contains putative SH2 and SH3 domain binding motifs and multiple LIM domains: identification of a vinculin and pp125Fak-binding region. J. Cell Sci. *107*, 1583–1591.

Way, J., and Chalfie, M. (1988). mec-3, a homeobox-containing gene that specifies differentiation of the touch receptor neurons in *C. elegans*. Cell *54*, 5–16.

Wessels, D., Soll, D.R., Knecht, D., Loomis, W.F., De Lozanne, A., and Spudich, J. (1988). Cell motility and chemotaxis in *Dictyostelium* amebae lacking myosin heavy chain. Dev. Biol. *128*, 164–177.

Westphal, M., Jungbluth, A., Heidecker, M., Muhlbauer, B., Heizer, C., Schwartz, J.M., Marriott, G., and Gerisch, G. (1997). Microfilament dynamics during cell movement and chemotaxis monitored using a GFP-actin fusion protein. Curr. Biol. *7*, 176–183.

Wu, L.J., Valkema, R., van Haastert, P.J.M., and Devreotes, P.N. (1995). The G protein beta subunit is essential for multiple responses to chemoattractants in *Dictyostelium*. J. Cell Biol. *129*, 1667–1675.